COUPLING IMPEDANCES OF MUFFIN–TIN STRUCTURES WITH CLOSED AND OPEN SIDES

M. Filtz
Technische Universität Berlin, EN–2, Einsteinufer 17, D–10587 Berlin

Abstract

In a previous work the eigenmodes of a muffin–tin structure limited with lateral electric walls were calculated using the mode matching technique. Now a modulated off axis beam is introduced and the beam induced fields, as well as the longitudinal coupling impedances are calculated. Furthermore, in order to get the fields in case of the open structure, the discrete set of modes in the field expansions was replaced by a continuous spectrum. The appearing Fourier integrals are determined by means of the residuum calculus.

I. INTRODUCTION

In [1] an analytical solution based on the mode matching technique was proposed for calculating the fields in a periodic muffin–tin structure. In order to obtain a discrete set of modes in the drift region, a closed structure with electric walls at $x = \pm(w+d)/2$ was assumed. If one chooses the distance d large enough, the influence may be neglegible for the resulting accelerating mode, but not for the deflecting mode, i.e. the dispersion relation for the deflecting mode depends strongly on the position of the electric walls. For example, if $d \to \infty$ one can expect that the cut–off frequency goes to zero. The purpose of the present paper is the extension of the previous analysis to an open structure (Fig. 1). Due to the lack of boundary conditions in x–direction, the fields in the drift region are now represented by a continuous spectrum of waveguide modes. The solution of this problem can be derived by utilizing the Fourier transform in combination with the mode matching technique.

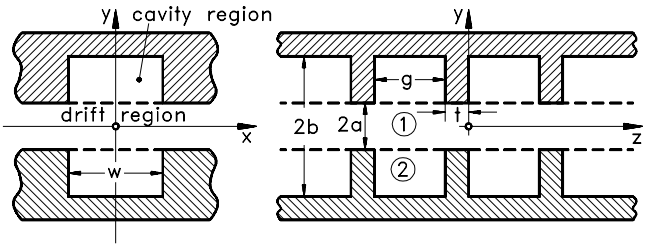

Figure 1. Transverse and longitudinal cut of the structure under consideration.

II. SOURCE FIELD IN THE DRIFT REGION

In order to determine the beam coupling impedances, we now introduce a charged particle $Q/2$ travelling off axis at $x = \delta x$, $y = \delta y$ with constant velocity $\mathbf{v} = \beta c\ \mathbf{e}_z$ in a parallel–plate waveguide. In the plane $y = 0$ we furthermore assume magnetic or electric boundary conditions (Fig. 2).

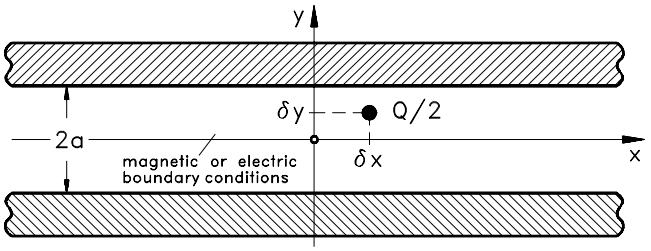

Figure 2. Charge $Q/2$ travelling in a parallel–plate waveguide.

In the frequency domain the magnetic field produced by this charge at $y = a$ can be written as the Fourier integral

$$H_x^{(s)} = -\frac{Q}{4\pi}\, \mathrm{e}^{-\mathrm{j}\frac{k}{\beta}z} \int_{-\infty}^{\infty} \mathrm{e}^{\mathrm{j}\xi(x-\delta x)} \frac{\mathrm{e}^{\eta\delta y} \pm \mathrm{e}^{-\eta\delta y}}{\mathrm{e}^{\eta a} \pm \mathrm{e}^{-\eta a}}\, \mathrm{d}\xi \qquad (1)$$

$$\eta = \sqrt{\left(\frac{k}{\gamma\beta}\right)^2 + \xi^2} \quad , \quad \gamma^2 = \frac{1}{1-\beta^2} \quad , \quad k = \frac{\omega}{c}$$

where the upper sign is valid for magnetic and the lower for electric boundary conditions at $y = 0$. Solving the Fourier integral by means of the residuum calculus one gets a different formulation

$$H_x^{(s)} = \frac{Q}{2a}\, \mathrm{e}^{-\mathrm{j}\frac{k}{\beta}z} \sum_i (-1)^i \left\{ \begin{array}{c} \cos p_i\delta y \\ \sin p_i\delta y \end{array} \right\} \mathrm{e}^{-\lambda|x-\delta x|} \qquad (2)$$

$$\lambda = \sqrt{p_i^2 + \left(\frac{k}{\gamma\beta}\right)^2} \quad , \quad p_i = \left\{ \begin{array}{ll} (2i-1)\pi/2a\ , & \mathrm{ma.} \\ i\pi/a\ , & \mathrm{el.} \end{array} \right.$$

which will be used as a source term in the following.

III. THE SCATTERED FIELD PRODUCED BY THE CAVITIES

The field in the cavities can be determined in terms of standing wave functions as was done in [1]. Hence, in this paragraph we will only discuss the field expansion in the drift region 1, which can be written in the form

$$\mathbf{E}_t^{(1)} = \frac{Z_0 Q}{2\pi} \sum_n \int_{-\infty}^{\infty} \mathbf{F}_n(\xi, x, z) V_n(\xi, y) A_n(\xi)\, \mathrm{d}\xi \qquad (3)$$

$$\mathbf{e}_y \times \mathbf{H}_t^{(1)} = \frac{Q}{2\pi} \sum_n \int_{-\infty}^{\infty} \mathbf{F}_n(\xi, x, z) V_n'(\xi, y) A_n(\xi) Y_n^{(1)}\, \mathrm{d}\xi$$

$$V_n(\xi, y) = \frac{-V_n^+(\xi, y) \mp V_n^-(\xi, y)}{V_n^+(\xi, a) \pm V_n^-(\xi, a)}\ , \ V_n' = \frac{-\mathrm{j}}{K_n^{(1)}(\xi)} \frac{\partial V_n}{\partial y}$$

$$V_n^{\pm}(\xi,y) = \exp\left\{\mp \mathrm{j}\, K_n^{(1)}(\xi) y\right\},\ K_n^{(1)}(\xi) = \sqrt{k^2-\beta_n^2-\xi^2}$$

$$Y_n^{(1)}(\xi) = \begin{cases} K_n^{(1)}(\xi)/k & ,\ TE_y \\ k/K_n^{(1)}(\xi) & ,\ TM_y \end{cases} \quad , \quad \beta_n = \frac{k}{\beta} + \frac{2\pi n}{g+t}$$

$$\mathbf{F}_n(\xi,x,z) = \mathrm{j}\, \mathrm{e}^{-\mathrm{j}(\beta_n z + \xi x)} \begin{cases} \beta_n \mathbf{e}_x - \xi\, \mathbf{e}_z & ,\ TE_y \\ -\xi\, \mathbf{e}_x - \beta_n \mathbf{e}_z & ,\ TM_y \end{cases}$$

As can be seen, the field is again decomposed in space harmonics with phase constants β_n and splitted into transverse electric (TE_y) and transverse magnetic (TM_y) components w.r.t $y = a$. The upper sign in V_n corresponds to a magnetic wall and the lower to an electric wall in $y = 0$. The main difference in Eq. (3) and the analogous field expansion in [1] is, that we now have to deal with an unknown continuous spectrum $A_n(\xi)$.

Due to lack of space, we will give only a brief summary of our analysis without mathematical details. Using the identity

$$\int_0^{g+t}\int_{-\infty}^{\infty} \mathbf{F}_n(\xi,x,z)\cdot\mathbf{F}_\nu^*(\xi',x,z)\,\mathrm{d}x\,\mathrm{d}z =$$

$$= 2\pi(g+t)\left\{\beta_n^2+\xi^2\right\}\delta(\xi-\xi')\delta_n^\nu \qquad (4)$$

and satisfying the boundary condition for the electric field, one can express the unknown spectrum $A_n(\xi)$ in terms of the discrete coefficients of the field expansion in the cavity region 2. Substituting this spectrum into the Fourier integral of the magnetic field this integral can be written in the form

$$I_\nu = (-1)^m I_\nu^I - I_\nu^{II} = \qquad (5)$$

$$= (-1)^m \int_{-\infty}^{\infty} f_\nu(\xi)\, \mathrm{e}^{-\mathrm{j}\xi(x-\frac{w}{2})}\,\mathrm{d}\xi - \int_{-\infty}^{\infty} f_\nu(\xi)\, \mathrm{e}^{-\mathrm{j}\xi(x+\frac{w}{2})}\,\mathrm{d}\xi\ .$$

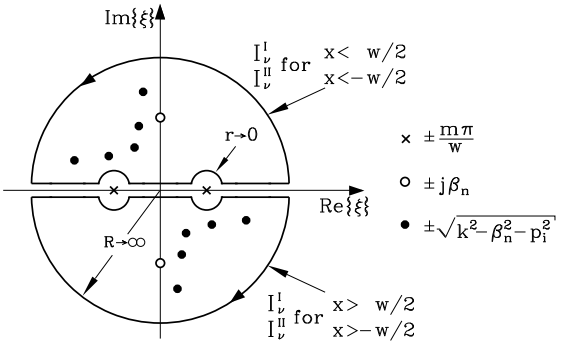

Figure 3. The location of poles in the complex plane.

The function $f_\nu(\xi)$ has poles at $\xi = \pm\frac{m\pi}{w}$, $\xi = \pm\mathrm{j}\ \beta_n$, $\xi = \pm\sqrt{k^2-\beta_n^2-p_i^2}$. It can easily be shown, that the poles $\xi = \pm\mathrm{j}\ \beta_n$ do not contribute, because they cancel each other after summing TE_y and TM_y modes. Fig. 3 shows the location of poles in the complex plane, and the integration path, where a complex wave number k with a small imaginary part was assumed. After solving the integral Eq. (5) by means of the residuum calculus, and satisfying the required continuity of the magnetic field, one finally gets a system of linear equations for the field coefficients in the cavity region.

IV. FINITE NUMBER OF CELLS

The analysis described above is valid for an infinite periodic structure. With a little modification however, we can use it to get results for a structure consisting of any finite number of cells. If we rotate the direction of the beam travelling along the structure by an angle of 90^o around the y–axis, and if we choose zero phase advance per cell, i.e. $\beta_n = 2\pi n/(g+t)$, then we obtain the fields produced by one single cell (Fig. 4).

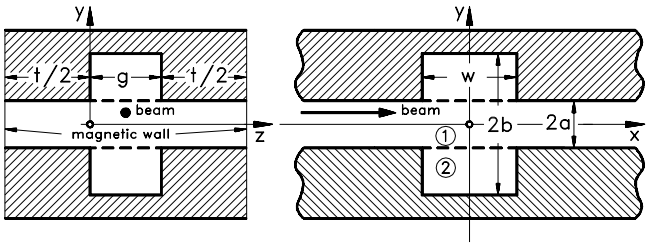

Figure 4. Changing the beam direction

As can be seen in Fig. 4, this manipulation leads to magnetic boundary conditions in the planes $z = -t/2$ and $z = g + t/2$, if the beam is located at $z = g/2$, $y = \delta y$. Of course, the meaning of dimension g has to be exchanged by w and vice versa. Adding more cells in x–direction is straightforward and leads to an increase of the number of linear equations by a factor of N, where N is the number of cells. Clearly, the structure is not exactly open. But it supports a TEM–wave, which radiates in beam direction and causes losses similar to those in a fully open structure.

V. NUMERICAL RESULTS

After solving the system of linear equations for the unknown field coefficients the integral

$$-Q\ Z(\omega) = \int_{z_1}^{z_2} E_z^{(1)}(x=\delta x, y=\delta y, z)\ \mathrm{e}^{-\mathrm{j}\frac{k}{\beta}z}\,\mathrm{d}z \qquad (6)$$

giving the longitudinal coupling impedance was evaluated, where $z_1 = 0$, $z_2 = g + t$ for an infinite periodic structure and $z_{1,2} = \mp\infty$ for a finite number of cells. Varying $\beta = v/c$ and looking for the peaks in Eq. (6), one obtains the dispersion relation which is plotted in Fig. 5 for the first deflecting mode, and compared to the closed structure analyzed in [1]. Obviously, the cut–off frequency goes to zero and there is no beam environment interaction for $\beta = 1$. Fig. 6+7 show the impedance of one single cell with electric or magnetic boundary conditions in $y = 0$, respectively. Below the cut–off frequency three sharp resonances can be observed. The following table gives their values in comparision to results from the FD computer code GDFIDL [3].

$\frac{f}{[\mathrm{GHz}]}$ (analytic)	120.0	223.4	243.1
$\frac{f}{[\mathrm{GHz}]}$ (GDFIDL)	120.1	223.2	241.8

The low frequency behaviour of the impedance in case of electric boundary conditions in $y = 0$, which allow the excitation of a TEM field, is similar to that calculated in [2] for a coaxial TEM structure, i.e. the imaginary part goes nearly linear with frequency and is much greater than the real one. Finally, in Fig. 8 the splitting up of the lowest cavity resonance

in a ten cell structure is demonstrated, where a small imaginary part of the wavenumber $k = \omega\sqrt{\varepsilon\mu} + j \cdot 10^{-4}$ was assumed. As can easily be recognized, the strongest resonances occure at about 122 GHz, which agrees very well with the $\frac{2\pi}{3}$ accelerating mode from the dispersion relation in [1].

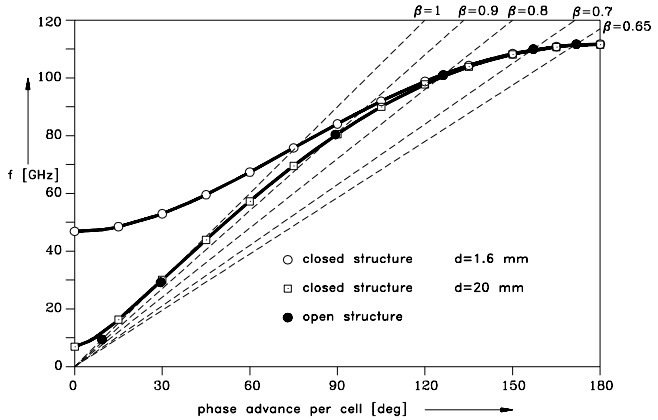

Figure 5. Dispersion relation for the first deflecting mode in a closed and open structure. ($a = 0.3$ mm, $b = 0.9$ mm, $w = 1.8$ mm, $g = 0.633$ mm, $t = 0.2$ mm)

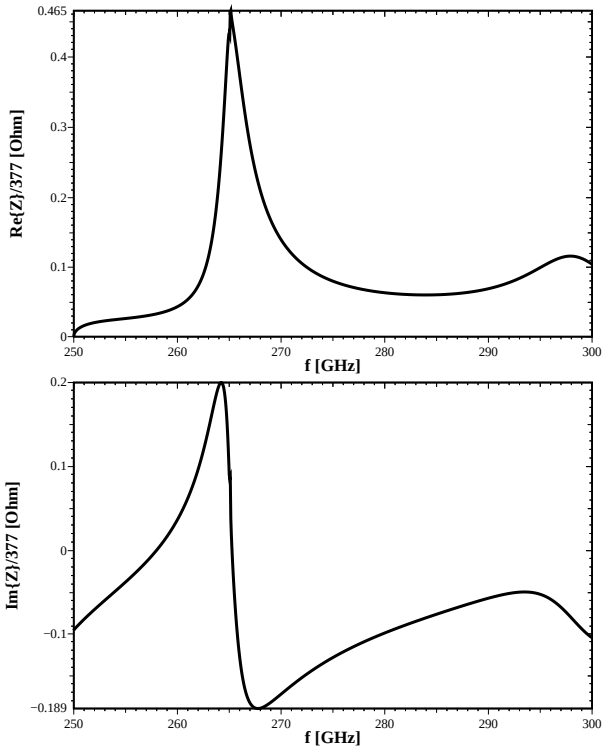

Figure 6. Longitudinal impedance of one single cell with no beam offset $\delta x = \delta y = 0$ and above cut–off frequency $f = 250$ GHz. ($a = 0.3$ mm, $b = 0.9$ mm, $w = 1.8$ mm, $g = 0.633$ mm, $d = 1.6$ mm)

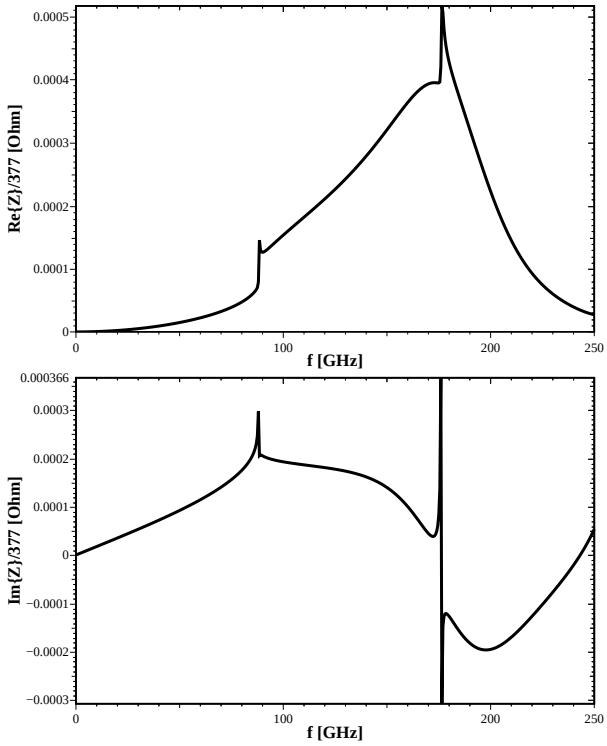

Figure 7. Longitudinal impedance of deflecting modes for a single cell with beam offset $\delta y = 0.01$ mm. ($a = 0.3$ mm, $b = 0.9$ mm, $w = 1.8$ mm, $g = 0.633$ mm, $d = 1.6$ mm)

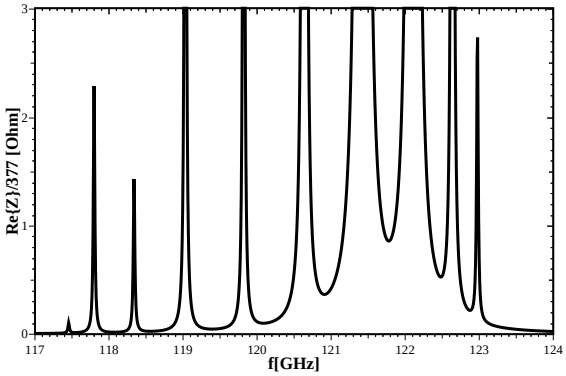

Figure 8. Real part of the longitudinal impedance per resonator for a ten cell structure with no beam offset. ($a = 0.3$ mm, $b = 0.9$ mm, $w = 1.8$ mm, $g = 0.633$ mm, $t = 0.2$ mm, $d = 1.6$ mm)

References

[1] M. Filtz,"Analytical Calculation of Waves in a Muffin–Tin Structure", Proc. of European Particle Accelerator Conf., London 1994, pp.1271–1273

[2] M. Filtz and T. Scholz,"Impedance Calculations for a Coaxial Liner", Proc. of European Particle Accelerator Conf., London 1994, pp.1333–1335

[3] W. Bruns, "GDFIDL: A Finite Difference Program for Arbitrarily Small Perturbations in Rectangular Geometries", to be presented at the COMPUMAG 95, Berlin